ACS Medicinal Chemistry Letters

pubs.acs.org/acsmedchemlett

Letter

Quantum Annealing Designs Nonhemolytic Antimicrobial Peptides in a Discrete Latent Space

Andrejs Tučs, Francois Berenger, Akiko Yumoto, Ryo Tamura, Takanori Uzawa,* and Koji Tsuda*

Cite This: *ACS Med. Chem. Lett.* 2023, 14, 577−582

Read Online

ACCESS | Metrics & More | Article Recommendations | Supporting Information

ABSTRACT: Increasing the variety of antimicrobial peptides is crucial in meeting the global challenge of multi-drug-resistant bacterial pathogens. While several deep-learning-based peptide design pipelines are reported, they may not be optimal in data efficiency. High efficiency requires a well-compressed latent space, where optimization is likely to fail due to numerous local minima. We present a multi-objective peptide design pipeline based on a discrete latent space and D-Wave quantum annealer with the aim of solving the local minima problem. To achieve multi-objective optimization, multiple peptide properties are encoded into a score using non-dominated sorting. Our pipeline is applied to design therapeutic peptides that are antimicrobial and non-hemolytic at the same time. From 200 000 peptides designed by our pipeline, four peptides proceeded to wet-lab validation. Three of them showed high anti-microbial activity, and two are non-hemolytic. Our results demonstrate how quantum-based optimizers can be taken advantage of in real-world medical studies.

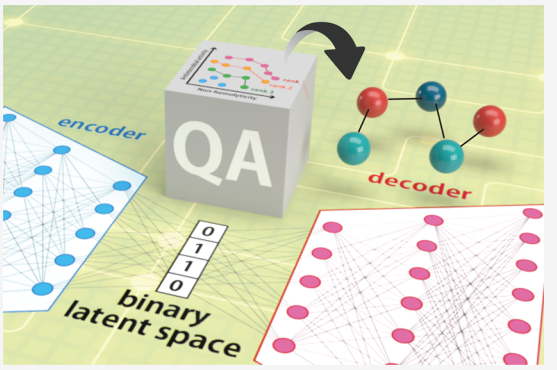

KEYWORDS: *Antimicrobial peptides, quantum annealing, deep learning, generative models*

Antibiotic resistance is an increasingly imminent threat to global health and food security, which is accelerated by misuse of antibiotics in humans and animals. It is expected that, by the year 2050, global deaths by drug-resistant pathogens will rise to 10 million.[1] Antimicrobial peptides (AMPs) are considered an effective means to solving the growing health problems related to drug-resistant pathogens, because microbes have been exposed to natural AMPs for millions of years, but widespread resistance to them is not yet reported.[2] Conventional development of AMPs is, however, struggling in dealing with the huge peptide sequence space. This situation motivated a series of studies of deep-learning-based AMP design. For example, Das et al.[3] employed a variational autoencoder with a continuous latent space and applied a Bayesian sampling method to the latent space to design AMPs. Capecchi et al.[4] used a deep-learning model based on recurrent neural networks to generate therapeutically favorable AMPs that are not likely to destroy red blood cells (i.e., non-hemolytic). Tucs et al.[5] employed a generative adversarial network (GAN) to create AMPs. Basically, these methods use the models developed for natural language processing where a tremendous amount of labeled data is available. The number of known AMPs in the databases[6−9] is on the order of 10^4, requiring a data-efficient approach.

In this paper, we present a multi-objective AMP design pipeline using a binary variational autoencoder (bVAE)[10] and a D-Wave quantum annealer[11] (Figure 1) and report wet-lab-confirmed discovery of non-hemolytic antimicrobial peptides. In a class of deep-learning models called variational autoencoders (VAEs),[12] two neural networks called an *encoder* and a *decoder* are used. The encoder transforms the input to a latent representation. The decoder takes a latent representation and returns a reconstruction. The loss function is defined to measure the difference between the input and the reconstruction. After training with a dataset, a VAE will be able to reconstruct any input approximately. A latent representation is typically a real-valued vector,[12] but bVAE uses a bit vector instead. By specifying a latent representation (i.e., a point in the latent space), one can generate a new entity as the output of the decoder. In this paper, we provide peptide sequences as the input so that a latent representation can be decoded into a peptide sequence.

A quantum annealer (QA) is designed to solve a specific discrete optimization problem, called QUBO (Quadratic Unconstrained Binary Optimization).[11,13] QUBO can be mapped to the Hamiltonian of an Ising model. This fact enables us to apply a variety of classical and quantum hardware to build QUBO optimizers.[14] Among them, the D-wave

Received: November 17, 2022
Accepted: April 10, 2023
Published: April 13, 2023

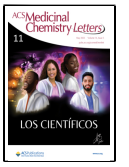

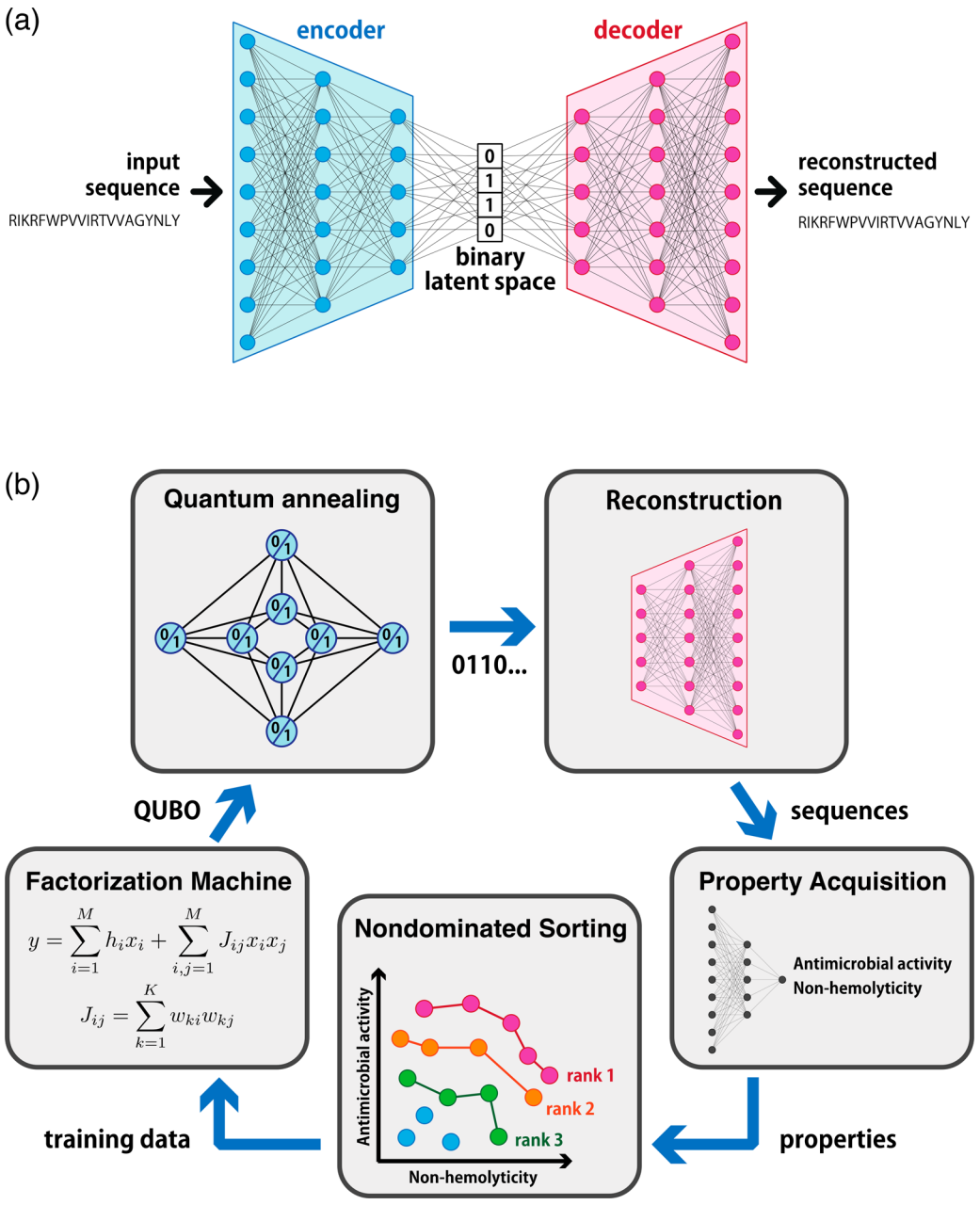

Figure 1. Peptide design pipeline. (a) A binary variational autoencoder is trained with a set of antimicrobial and non-antimicrobial peptide sequences. The autoencoder is trained to reconstruct the input sequence as accurately as possible. After the training, the decoder can map a bit vector (i.e., latent space representation) to a peptide sequence. (b) In our pipeline, bit vectors sampled from the quantum annealer are mapped to peptide sequences by the decoder. For these sequences, antimicrobial activity and non-hemolyticity are predicted. These two properties are summarized to a score with non-dominated sorting. A factorization machine is trained with the bit vectors and corresponding scores, and the quantum annealer is applied again to the trained factorization machine. The loop continues until the pre-determined number of peptides is obtained.

quantum annealer[11] is a widely used piece of hardware based on modulation of quantum fluctuations on superconducting qubits. What makes a QA attractive is the theoretical guarantee of finding the global optimal solution under the assumption of ideal qubits and slow annealing.[13] Although this goal is not attainable currently, recent successful case studies in materials science[15,16] imply that the quality of qubits has improved to the point that they are practically useful. In addition, QA-based methods are likely to benefit from future development of quantum technologies.

In the first stage of our pipeline (Figure 1a), bVAE is trained with known sequences. The second stage of designing peptides starts with a small set of peptides (Figure 1b). The sequences are mapped to bit vectors using the trained encoder. Multiple properties such as antimicrobial activity and hemolyticity are predicted by machine-learning models and summarized into a score via non-dominated sorting,[17] where each peptide is scored by a distance from the Pareto front. Note that the Pareto front is defined as the set of non-dominated solutions where no property can be improved without sacrificing the other at each solution.[18] Then, a factorization machine (FM)[19]

https://doi.org/10.1021/acsmedchemlett.2c00487
ACS Med. Chem. Lett. 2023, 14, 577−582

is trained with the pairs of bit vectors and scores. A quantum annealer is employed to optimize the FM prediction score, and the solutions are decoded to peptides using the decoder of bVAE. Properties of the new peptides are acquired by the prediction models, and the training set is expanded. This loop allows us to explore the sequence space efficiently by means of a highly compressed latent space and a powerful optimizer.

In the following, we present our peptide design pipeline called MOQA (Multi-objective Optimization by Quantum Annealing). First, we need to train two kinds of machine learning models: (1) binary VAE and (2) property predictors. We collected 19 530 antimicrobial and 5583 non-antimicrobial peptide sequences from APD,[8] CAMP,[7] LAMP,[9] DBAASP,[6] and YADAMP[20] databases. The antimicrobial and non-antimicrobial sequences are used to train a binary VAE with a 64-dimensional latent space for 400 epochs. We used the bVAE implementation by Baynazarov and Piontkovskaya.[21] To predict antimicrobial activity, a deep-learning model with a gated recurrent unit is trained. See Tucs et al.[5] for details of the predictor. As the hemolyticity predictor, an L2-regularized logistic regressor was trained with 2677 sequences from the DBAASP database. A sequence is labeled non-hemolytic if it causes less than 10% hemolysis at a concentration of at least 100 μM. See section 1 in the SI for details.

By using the encoder of bVAE, all peptides are translated to binary vectors. Our idea is to design a new binary vector using a quantum annealer that is later decoded back to a peptide. Let x_i (I = 1, ..., M) denote the binary vectors and $y_i^{(1)}$ and $y_i^{(2)}$ denote the antimicrobial activity and hemolyticity obtained by the predictors, respectively. These two properties are combined into a score y_i by means of *rank* obtained by non-dominated sorting. The samples at the Pareto front are assigned rank 1. After removing rank 1 samples, we obtain the Pareto front of the remaining samples, and those on the new front are assigned rank 2. This is repeated until all of the samples have their ranks. With a tunable parameter t, the score of a peptide of rank r is defined as $y = -1/r$ ($r \le t$), 10 ($r > t$). The parameter t is set to 20 initially.

The dataset $D = (x_i, y_i)$ where i = 1, ...M is used to train a factorization machine (FM). The functional form of a FM is described as

$$y = \sum_{i=1}^{M} h_i x_i + \sum_{i,j=1}^{M} \sum_{k=1}^{K} w_{ki} w_{kj} x_i x_j \quad (1)$$

where the weight matrix of quadratic terms is a low-rank matrix parameterized by w_{ki}. Given a training set, the FM is trained by minimizing the squared loss by libFM.[19] In the following experiments, the rank K is set to eight. After the parameters are fixed, a D-wave quantum annealer is applied to find the solutions minimizing eq 1. Due to noise, it is not always possible to attain the global optimal solution. We obtain a batch of 10 solutions from the quantum annealer at a time. These solutions are decoded to peptides, and their antimicrobial activity and hemolyticity are predicted. They are then added to the dataset D, and the non-dominated sorting scores are updated. The FM is retrained with the expanded dataset, and a next batch of solutions is obtained by the quantum annealer. This procedure is repeated until the predetermined number of peptides is generated. Notice that the parameter t is reduced by one whenever 100 sequences are generated. It allows our FM model to pay increasing attention to the Pareto front. It is a reasonable choice, because the Pareto front obtained in early iterations is not accurate and the score should be less sensitive to the rank.

Before solving our main peptide design problem, we benchmarked our pipeline in optimizing three easily computable properties (charge density, instability index, and Boman index). In computing these properties, we used Python package modlAMP[22] instead of predictors. The performance of our pipeline was measured by Pareto hyper-volume,[23] defined as the volume of a convex hull containing the origin and Pareto front. Figure 2 shows the distribution of Pareto hypervolume in

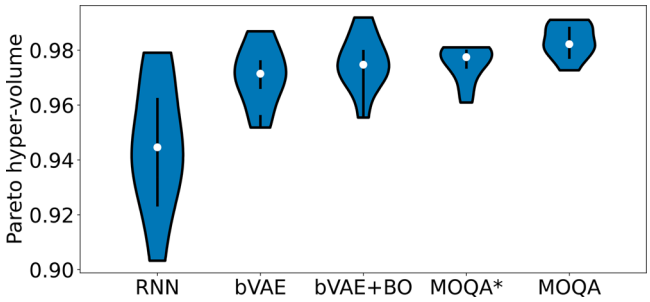

Figure 2. Benchmarking. Multi-objective optimization methods are compared in terms of Pareto hypervolume with 2000 samples. RNN represents the recurrent neural network used by Capecchi et al.[4] bVAE represents random selection in the latent space of bVAE. bVAE +BO represents Bayesian optimization on 100 000 randomly sampled sequences. MOQA and MOQA* represent our pipeline with adaptive tuning and with fixed rank t = 20, respectively. The distributions over 10 experiments are shown.

10 attempts of sampling 2000 sequences. We compared MOQA with MOQA*, i.e., the alternative pipeline with fixed rank t = 20, Bayesian optimization[24] on 100 000 randomly sampled sequences (i.e., bVAE+BO), random selection in the latent space of bVAE (i.e., bVAE), and the recurrent neural network used by Capecchi et al.[4] (i.e., RNN). See Figure S1 for the change of Pareto hypervolume with respect to the number of samples and Figure S2 for the results of individual properties. MOQA performed significantly better than RNN and Bayesian optimization, showing that MOQA is competitive with existing approaches.[25] MOQA was shown to be more effective than MOQA*, indicating the importance of taking Pareto-front uncertainty into account. Adaptive tuning allows the pipeline to put more emphasis on expanding the Pareto front, as the Pareto front is more accurately estimated.

A total of 200 000 peptide sequences are generated by MOQA in 10 independent runs. D-Wave Advantage (system 4.1) was used, and the dimensionality of the latent space was set to 64. We selected 75 sequences satisfying the following constraints. (1) The sequence does not have three consecutive amino acids. (2) Less than 50% of the amino acids in the sequence are hydrophobic. (3) The prediction probability of the CAMP server[7] is larger than 0.999. In addition, we used CAMPsign[26] to identify family-specific sequence signatures. Four sequences with more than two signatures were selected for experimental validation (Table 1).

We evaluated the antimicrobial activity of our peptides based on minimum inhibitory concentration (MIC) against *E. coli*. MIC is determined as the minimum concentration of an antimicrobial at which the growth of a target microbial is suppressed. See section 3 in the SI for details. No unexpected or unusually high safety hazards were encountered. As shown in Figure 3a, three out of four peptides exhibited effective

https://doi.org/10.1021/acsmedchemlett.2c00487
ACS Med. Chem. Lett. 2023, 14, 577−582

Table 1. Peptides Selected for Experimental Validation

ID	sequence	MIC (μg/mL)	hemolyticity
TA2-1	GFKTLKNLAKKVAKKVLKAVR	6.25	non-hemolytic
TA2-2	KLGKKILKKVGKHVGKFYTGII	6.25	non-hemolytic
TA2-3	WKSVLKKVIKGIGKVVSKVMGQAQ	3.13	hemolytic
TA2-4	GLVTVLKKVAKGIVKTASKVGSKEL	>100	N/A
ampicillin[a]	N/A	6.25	N/A

[a]Ampicillin is a commonly used antibiotic shown here for reference.

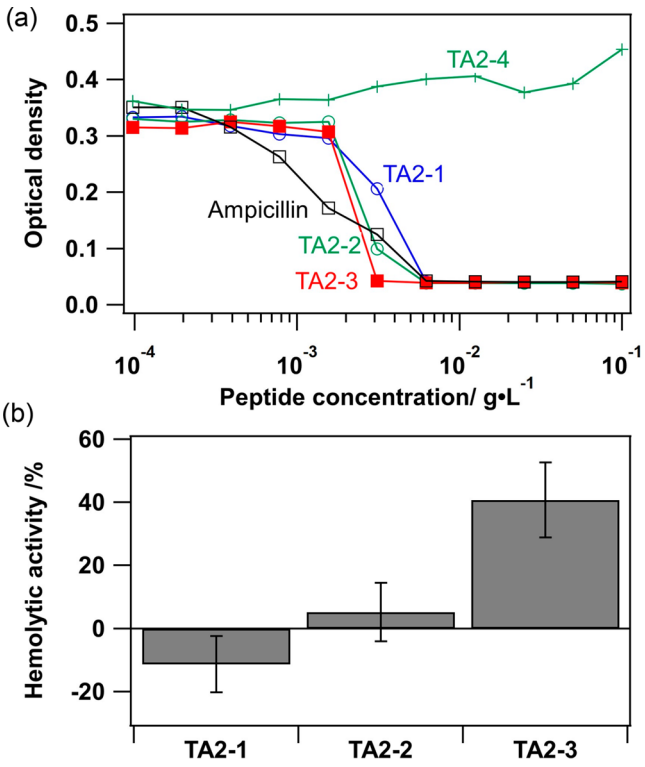

Figure 3. Experimental validation. (a) Optical density in microdilution assays against peptide concentration. (b) Hemolytic activity at 100 μM after 6 h. Error bars indicate variation over three experiments.

antimicrobial activity. Among them, TA2-3 exhibited the best antimicrobial performance, 3.1 μg/ML, which is twice better than that of a well-known antimicrobial, ampicillin (6.25 μg/ML). TA2-1 and TA2-2 were also highly active. We also conducted negative control experiments with 10 peptides created from randomly chosen points in the latent space. They did not show notable antimicrobial activities.

The hemolytic activity of the peptides was assayed by spectrophotometrically measuring hemoglobin released from red blood cells. Let us denote by h, h_{pos}, and h_{neg} the amount of released hemoglobin in the sample of interest and in the positive and negative controls, respectively. The hemolytic activity is defined as $(h - h_{neg})/(h_{pos} - h_{neg})$. See section 4 in the SI for details. Even at a high peptide concentration of 100 μM and a long incubation time of 6 h, TA2-1 and TA2-2 showed effectively no hemolytic activity, suggesting that these peptides are therapeutically viable (Figure 3b). TA2-3 showed relatively high activity of around 40%; hence it is less favorable therapeutically. This activity is, however, considered modest in comparison to the strong activity of naturally existing hemolytic peptide, melittin, that exhibits over 90% hemolytic activity in 1 h at 1 μM peptide concentration.[27]

We presented a peptide design pipeline consisting of quantum annealing and several machine-learning models and reported successful discovery of two non-hemolytic antimicrobial peptides. Our pipeline has room for improvement with respect to the following points: the accuracy of the predictors should be improved as much as possible; the factorization machine may not be the optimal choice as a surrogate model; the quantum annealer does not always optimize the objective function completely. Nevertheless, multiple successes in experimental validation show that our pipeline is working in practice.

In most cases, the number of possible synthesis experiments is limited due to available resources. We stopped our pipeline after generating 200 000 sequences and selecting four peptides for synthesis. If a user had more resources, it would be possible to continue generating more sequences. Our pipeline may be evaluated by the hit rate, i.e., the number of generated sequences to obtain a qualifying peptide. According to our synthesis experiments, the hit rate is estimated as 1/100 000. However, this estimate is quite rough.

Quantum annealing has been shown to be superior to classical simulated annealing in theory,[13] but the results of experimental comparison using the D-Wave quantum annealer are mixed (see Yaacoby et al.[28] and references therein). For example, Denchev et al.[29] showed that the quantum annealer is more efficient than simulated annealing in randomly generated problems, while Vert et al.[30] reported that the quantum annealer performed worse than simulated annealing in hard instances of bipartite matching problems. As mentioned earlier, however, qubit technologies are still in rapid development, and the optimization capability of quantum annealing is expected to improve. Our pipeline can be coupled with other Ising machines[14] such as a coherent Ising machine[31] or driven by a quantum approximate optimization algorithm[32] (QAOA) implemented on gate-based quantum computers. Our results are a first step toward expanding the application domain of quantum computing from routine optimization problems[33] such as the traveling salesman problem and graph coloring to real-world medical problems. Since bVAE can easily be modified to generate images, strings, and graphs,[10] our pipeline has the potential to be applied to a wide range of biological, chemical, and pharmaceutical design problems. Hopefully, our work serves as a stepping stone to successful and pervasive employment of quantum technologies in medical research.

■ ASSOCIATED CONTENT

Data Availability Statement

The code of MOQA is available at https://github.com/tucs7/MOQA.

Supporting Information

The Supporting Information is available free of charge at https://pubs.acs.org/doi/10.1021/acsmedchemlett.2c00487.

https://doi.org/10.1021/acsmedchemlett.2c00487
ACS Med. Chem. Lett. 2023, 14, 577−582

Section 1, details about the hemolyticity predictor; section 2, description of the negative control experiments; sections 3 and 4, experimental details about peptide synthesis and measurement; Figure S1, optimization results of multi-objective peptide design; Figure S2, results of optimizing individual properties (PDF)

AUTHOR INFORMATION

Corresponding Authors

Takanori Uzawa − *Emergent Bioengineering Materials Research Team, RIKEN Center for Emergent Matter Science, Wako, Saitama 351-0198, Japan; Nano Medical Engineering Laboratory, RIKEN Cluster for Pioneering Research, Wako, Saitama 351-0198, Japan;* orcid.org/0000-0001-6042-513X; Email: tuzawa@riken.jp

Koji Tsuda − *Graduate School of Frontier Sciences, The University of Tokyo, Kashiwa, Chiba 277-8561, Japan; Research and Services Division of Materials Data and Integrated System, National Institute for Materials Science (NIMS), Tsukuba 305-0044, Japan; RIKEN Center for Advanced Intelligence Project, RIKEN, Chuo-ku, Tokyo 103-0027, Japan;* orcid.org/0000-0002-4288-1606; Email: tsuda@k.u-tokyo.ac.jp

Authors

Andrejs Tučs − *Graduate School of Frontier Sciences, The University of Tokyo, Kashiwa, Chiba 277-8561, Japan*

Francois Berenger − *Graduate School of Frontier Sciences, The University of Tokyo, Kashiwa, Chiba 277-8561, Japan;* orcid.org/0000-0003-1377-944X

Akiko Yumoto − *Emergent Bioengineering Materials Research Team, RIKEN Center for Emergent Matter Science, Wako, Saitama 351-0198, Japan*

Ryo Tamura − *Graduate School of Frontier Sciences, The University of Tokyo, Kashiwa, Chiba 277-8561, Japan; International Center for Materials Nanoarchitectonics (WPI-MANA), National Institute for Materials Science (NIMS), Tsukuba 305−0044, Japan; Research and Services Division of Materials Data and Integrated System, National Institute for Materials Science (NIMS), Tsukuba 305-0044, Japan; RIKEN Center for Advanced Intelligence Project, RIKEN, Chuo-ku, Tokyo 103-0027, Japan;* orcid.org/0000-0002-0349-358X

Complete contact information is available at: https://pubs.acs.org/10.1021/acsmedchemlett.2c00487

Author Contributions

K.T. and R.T. conceived the idea and designed the research. A.T. and F.B. developed the pipeline and evaluated it. A.Y. and T.U. conducted the biological experiments. K.T. and T.U. planned and supervised the project. All members contributed to the preparation of the manuscript.

Notes

The authors declare no competing financial interest.

ACKNOWLEDGMENTS

This work is supported by RIKEN engineering network fund, AMED JP20nk0101111 and JP19fk0108158h0001, NEDO P15009, SIP (Technologies for Smart Bioindustry and Agriculture), JST ERATO JPMJER1903, and JST CREST JPMJCR21O2

REFERENCES

(1) O'Neill, J. *Antimicrobial Resistance: Tackling a Crisis for the Health and Wealth of Nations*; Wellcome Trust, 2014.

(2) Fjell, C. D.; Hiss, J. A.; Hancock, R. E.; Schneider, G. Designing antimicrobial peptides: form follows function. *Nat. Rev. Drug Discov.* **2012**, *11* (1), 37−51.

(3) Das, P.; Sercu, T.; Wadhawan, K.; Padhi, I.; Gehrmann, S.; Cipcigan, F.; Chenthamarakshan, V.; Strobelt, H.; dos Santos, C.; Chen, P.-Y.; Yang, Y. Y.; Tan, J. P. K.; Hedrick, J.; Crain, J.; Mojsilovic, A. Accelerated antimicrobial discovery via deep generative models and molecular dynamics simulations. *Nat. Biomed. Eng.* **2021**, *5* (6), 613−623.

(4) Capecchi, A.; Cai, X.; Personne, H.; Köhler, T.; van Delden, C.; Reymond, J.-L. Machine learning designs non-hemolytic antimicrobial peptides. *Chem. Sci.* **2021**, *12* (26), 9221−9232.

(5) Tucs, A.; Tran, D. P.; Yumoto, A.; Ito, Y.; Uzawa, T.; Tsuda, K. Generating Ampicillin-Level Antimicrobial Peptides with Activity-Aware Generative Adversarial Networks. *ACS Omega* **2020**, *5* (36), 22847−22851.

(6) Pirtskhalava, M.; Gabrielian, A.; Cruz, P.; Griggs, H. L.; Squires, R. B.; Hurt, D. E.; Grigolava, M.; Chubinidze, M.; Gogoladze, G.; Vishnepolsky, B.; Alekseev, V.; Rosenthal, A.; Tartakovsky, M. DBAASP v.2: an enhanced database of structure and antimicrobial/cytotoxic activity of natural and synthetic peptides. *Nucleic Acids Res.* **2016**, *44* (D1), D1104−D1112.

(7) Waghu, F. H.; Gopi, L.; Barai, R. S.; Ramteke, P.; Nizami, B.; Idicula-Thomas, S. CAMP: Collection of sequences and structures of antimicrobial peptides. *Nucleic Acids Res.* **2014**, *42* (D1), D1154−D1158.

(8) Wang, Z.; Wang, G. APD: the Antimicrobial Peptide Database. *Nucleic Acids Res.* **2004**, *32*, D590−D592.

(9) Zhao, X.; Wu, H.; Lu, H.; Li, G.; Huang, Q. LAMP: A Database Linking Antimicrobial Peptides. *PLoS One* **2013**, *8* (6), e66557.

(10) Jang, E.; Gu, S.; Poole, B. Categorical Reparameterization with Gumbel-Softmax. *arXiv Preprint* **2016**, 1611.01144.

(11) Johnson, M. W.; Amin, M. H. S.; Gildert, S.; Lanting, T.; Hamze, F.; Dickson, N.; Harris, R.; Berkley, A. J.; Johansson, J.; Bunyk, P.; Chapple, E. M.; Enderud, C.; Hilton, J. P.; Karimi, K.; Ladizinsky, E.; Ladizinsky, N.; Oh, T.; Perminov, I.; Rich, C.; Thom, M. C.; Tolkacheva, E.; Truncik, C. J. S.; Uchaikin, S.; Wang, J.; Wilson, B.; Rose, G. Quantum annealing with manufactured spins. *Nature* **2011**, *473* (7346), 194−198.

(12) Kingma, D. P.; Welling, M. Auto-Encoding Variational Bayes. *arXiv Preprint* **2013**, 1312.6114.

(13) Kadowaki, T.; Nishimori, H. Quantum annealing in the transverse Ising model. *Phys. Rev. E* **1998**, *58* (5), 5355−5363.

(14) Mohseni, N.; McMahon, P. L.; Byrnes, T. Ising machines as hardware solvers of combinatorial optimization problems. *Nat. Rev. Phys.* **2022**, *4* (6), 363−379.

(15) Wilson, B. A.; Kudyshev, Z. A.; Kildishev, A. V.; Kais, S.; Shalaev, V. M.; Boltasseva, A. Machine learning framework for quantum sampling of highly constrained, continuous optimization problems. *Appl. Phys. Rev.* **2021**, *8* (4), 041418.

(16) Kitai, K.; Guo, J.; Ju, S.; Tanaka, S.; Tsuda, K.; Shiomi, J.; Tamura, R. Designing metamaterials with quantum annealing and factorization machines. *Phys. Rev. Res.* **2020**, *2* (1), 013319.

(17) Deb, K.; Pratap, A.; Agarwal, S.; Meyarivan, T. A fast and elitist multiobjective genetic algorithm: NSGA-II. *IEEE Trans. Evol. Comput.* **2002**, *6* (2), 182−197.

(18) Miettinen, K. *Nonlinear Multiobjective Optimization*; Kluwer Academic Publishers, 1999.

(19) Rendle, S. Factorization Machines with libFM. *ACM Trans. Intell. Syst. Tech.* **2012**, *3* (3), 1−22.

(20) Piotto, S. P.; Sessa, L.; Concilio, S.; Iannelli, P. YADAMP: yet another database of antimicrobial peptides. *Int. J. Antimicrob. Agents* **2012**, *39* (4), 346−351.

(21) Baynazarov, R.; Piontkovskaya, I. Binary Autoencoder for Text Modeling. *Artificial Intelligence and Natural Language*; Communications in Computer and Information Science, 2019; pp 139−150.

(22) Muller, A. T; Gabernet, G.; Hiss, J. A; Schneider, G. modlAMP: Python for antimicrobial peptides. *Bioinformatics* **2017**, *33* (17), 2753−2755.
(23) Couckuyt, I.; Deschrijver, D.; Dhaene, T. Fast calculation of multiobjective probability of improvement and expected improvement criteria for Pareto optimization. *J. Glob. Optim.* **2014**, *60* (3), 575−594.
(24) Motoyama, Y.; Tamura, R.; Yoshimi, K.; Terayama, K.; Ueno, T.; Tsuda, K. Bayesian optimization package: PHYSBO. *Comput. Phys. Commun.* **2022**, *278*, 108405.
(25) Terayama, K.; Sumita, M.; Tamura, R.; Tsuda, K. Black-Box Optimization for Automated Discovery. *Acc. Chem. Res.* **2021**, *54* (6), 1334−1346.
(26) Waghu, F. H.; Barai, R. S.; Idicula-Thomas, S. Leveraging family-specific signatures for AMP discovery and high-throughput annotation. *Sci. Rep.* **2016**, *6* (1), 24684 DOI: 10.1038/srep24684.
(27) DeGrado, W. F.; Musso, G. F.; Lieber, M.; Kaiser, E. T.; Kézdy, F. J. Kinetics and mechanism of hemolysis induced by melittin and by a synthetic melittin analogue. *Biophys. J.* **1982**, *37* (1), 329−338.
(28) Yaacoby, R.; Schaar, N.; Kellerhals, L.; Raz, O.; Hermelin, D.; Pugatch, R. Comparison between a quantum annealer and a classical approximation algorithm for computing the ground state of an Ising spin glass. *Phys. Rev. E* **2022**, *105* (3), 035305 DOI: 10.1103/PhysRevE.105.035305.
(29) Denchev, V. S.; Boixo, S.; Isakov, S. V.; Ding, N.; Babbush, R.; Smelyanskiy, V.; Martinis, J.; Neven, H. What is the Computational Value of Finite-Range Tunneling? *Phys. Rev. X* **2016**, *6* (3), 031015.
(30) Vert, D.; Sirdey, R.; Louise, S. Benchmarking Quantum Annealing Against "Hard" Instances of the Bipartite Matching Problem. *SN Comput. Sci.* **2021**, *2* (2), 106.
(31) Inagaki, T.; Haribara, Y.; Igarashi, K.; Sonobe, T.; Tamate, S.; Honjo, T.; Marandi, A.; McMahon, P. L.; Umeki, T.; Enbutsu, K.; Tadanaga, O.; Takenouchi, H.; Aihara, K.; Kawarabayashi, K.-i.; Inoue, K.; Utsunomiya, S.; Takesue, H. A coherent Ising machine for 2000-node optimization problems. *Science* **2016**, *354* (6312), 603−606.
(32) Farhi, E.; Goldstone, J.; Gutmann, S. A Quantum Approximate Optimization Algorithm. *arXiv Preprint* **2014**, 1411.4028.
(33) Kochenberger, G.; Hao, J.-K.; Glover, F.; Lewis, M.; Lü, Z.; Wang, H.; Wang, Y. The unconstrained binary quadratic programming problem: a survey. *J. Comb. Optim.* **2014**, *28* (1), 58−81.

https://doi.org/10.1021/acsmedchemlett.2c00487
ACS Med. Chem. Lett. 2023, 14, 577−582